The American Journal of Pathology, Vol. 183, No. 6, December 2013

ELSEVIER

The American Journal of PATHOLOGY

ajp.amjpathol.org

ANIMAL MODELS

Hepatic Loss of miR-122 Predisposes Mice to Hepatobiliary Cyst and Hepatocellular Carcinoma upon Diethylnitrosamine Exposure

Shu-hao Hsu,[*†] Bo Wang,[*†] Huban Kutay,[‡] Hemant Bid,[‡§] Julia Shreve,[‡] Xiaoli Zhang,[‡¶] Stefan Costinean,[‖] Anna Bratasz,[‡] Peter Houghton,[‡§] and Kalpana Ghoshal[*§‖**]

From the Departments of Molecular and Cellular Biochemistry and Pathology,[‖] the Molecular, Cellular and Developmental Biology Program,[†] the Comprehensive Cancer Center,[‡] The Ohio State University, Columbus; the Center for Childhood Cancer,[§] Nationwide Children's Hospital, Columbus; the Center for Biostatistics,[¶] The Ohio State University, Columbus; and the Experimental Therapeutics Program,** College of Medicine, The Ohio State University, Columbus, Ohio*

Accepted for publication August 7, 2013.

Address correspondence to Kalpana Ghoshal, Ph.D., Department of Pathology, The Ohio State University, 646C TMRF, 420 W. 12th Av, Columbus, OH 43210. E-mail: Kalpana.Ghoshal@osumc.edu.

Loss of miR-122 causes chronic steatohepatitis and spontaneous hepatocellular carcinoma. However, the consequence of miR-122 deficiency on genotoxic stress—induced liver pathogenesis is poorly understood. Here, we investigated the impact of miR-122 depletion on liver pathobiology by treating liver-specific miR-122 knockout (LKO) mice with the hepatocarcinogen diethylnitrosamine (DEN). At 25 weeks post-DEN injection, all LKO mice developed CK-19—positive hepatobiliary cysts, which correlated with DEN-induced transcriptional activation of *Cdc25a* mediated through E2f1. Additionally, LKO livers were more fibrotic and vascular, and developed larger microscopic tumors, possibly due to elevation of the *Axl* oncogene, a receptor tyrosine kinase as a novel target of miR-122, and several protumorigenic miR-122 targets. At 35 weeks following DEN exposure, LKO mice exhibited a higher incidence of macroscopic liver tumors (71%) and cysts (86%) compared to a 21.4% and 0% incidence of tumors and cysts, respectively, in control mice. The tumors in LKO mice were bigger (ninefold, $P = 0.015$) and predominantly hepatocellular carcinoma, whereas control mice mostly developed hepatocellular adenoma. DEN treatment also reduced survival of LKO mice compared to control mice ($P = 0.03$). Interestingly, induction of oxidative stress and proinflammatory cytokines in LKO liver shortly after DEN exposure indicates predisposition of a pro-tumorigenic microenvironment. Collectively, miR-122 depletion facilitates cystogenesis and hepatocarcinogenesis in mice on DEN challenge by upregulating several genes involved in proliferation, growth factor signaling, neovascularization, and metastasis. *(Am J Pathol 2013, 183: 1719—1730; http://dx.doi.org/10.1016/j.ajpath.2013.08.004)*

Hepatocellular carcinoma (HCC) is the most common liver cancer, and the fifth most prevalent cancer worldwide. Its incidence has almost tripled in the United States during the past 20 years.[1,2] Almost all HCC arises in patients with chronic liver disease and cirrhosis. The difficulties in early diagnosis and the lack of effective therapy are responsible for the fast-growing mortality of HCC patients. Therefore, development of novel biomarkers for early detection and a therapeutic strategy to treat this deadly disease in a timely manner are urgently needed. Although the major risk factor leading to HCC is hepatitis B and C virus infection, alcoholic and nonalcoholic fatty liver disease are emerging as important risk factors for HCC.[3] Additionally, genetic mutations, such as hemochromatosis, α-1-antitrypsin deficiency, and environmental toxins such as aflatoxin B1 and vinyl chloride also cause liver cancer. It is, therefore, important to investigate the impact of specific gene/environment interactions on hepatocarcinogenesis because disruption of specific genes can profoundly influence the response of an organism to genotoxic insults.

miR-122 is an abundant liver-specific miRNA that is conserved in vertebrates.[4] miR-122 is transcribed as an

Supported by NIH grants DK088076 and CA086978 (K.G.).

http://dx.doi.org/10.1016/j.ajpath.2013.08.004

approximately 7.5-kiloneucleotide (knt) primary transcript from an intergenic region, which is subsequently processed to 66-nt precursor RNA and approximately 22-nt mature miR-122. Hepatocyte-specific transcription of miR-122 is regulated by liver-enriched transcription factors such as hepatocyte nuclear factor-1-α (HNF1α), HNF3α/β,[5] HNF4,[6] and HNF6.[7] Interestingly, the expression of the primary transcript, but not the mature miR-122, oscillates with diurnal rhythm regulated by the repressor Rev-erbA.[8] Stabilization of mature miR-122 by the addition of a single adenosine to its 3′-end by GLD2, a noncanonical cytoplasmic poly(A) polymerase,[9] is likely to cause its high abundance.

miR-122 is one of the most widely studied miRNAs.[4] Several seminal discoveries were made while studying its physiological function, HCV viral infection, and cancer. miR-122 was successfully depleted in the livers of mice by injecting antagomir, a cholesterol-conjugated, phosphorothioate-modified antisense oligonucleotide, through the tail vein, which resulted in hypocholesterolemia,[10] suggesting its potential use in the treatment of atherosclerosis. Another unique function of miR-122 is its role in aiding HCV replication in hepatocytes. Because of the high abundance of miR-122 only in the liver, HCV virus can propagate only in liver, causing hepatitis, which often leads to HCC. Miravirsen, a locked nucleic acid−modified 15-mer anti−miR-122 oligonucleotide, is the first miRNA-based therapy currently undergoing clinical trials in reducing viremia in HCV-infected patients. However, several studies have shown that prolonged depletion of miR-122 can cause deleterious effects on liver functions. First, miR-122 was down-regulated in primary HCC of both rodent and human origin,[11] which correlated with poor prognosis, metastasis, and dedifferentiation of hepatocytes.[5] Second, miR-122 exhibited tumor suppressor function when ectopically expressed in HCC cell lines.[12,13] Third, miravirsen-mediated depletion of miR-122 caused systemic iron deficiency in adult mice.[14] Finally, progressive development of hepatitis, steatosis, and fibrosis in liver-specific and germline miR-122 knockout mice reinforces its essential role in maintaining liver function.[15,16] Furthermore, occurrence of spontaneous liver tumors in approximately 50% of the male mice after 12 months, and profound reduction of liver tumor growth after delivery of the *miR-122* precursor gene[15] or miR-122 mimic[12,17] in mice confirmed its tumor suppressor function, and suggested that prolonged depletion of miR-122 in HCC patients might have deleterious consequences. These observations revealed that this miRNA is not essential for liver development, although it performs diverse functions in the liver.

In the present study, we investigated susceptibility of liver-specific miR-122 knockout (LKO) mice to diethylnitrosamine (DEN), the most frequently used carcinogen that promotes liver tumors in rodents. The results show that the loss of hepatic miR-122 predisposes mice to develop liver cysts and HCCs within 8 months on challenge with this hepatocarcinogen during the neonatal stage.

Materials and Methods

Mice

LKO mice were generated by crossing floxed (miR-122$^{loxP/loxP}$) mice with transgenic *Alb-Cre* mice, obtained from the Jackson Laboratory (Bar Harbor, ME).[15] The mice were housed in barrier facilities and fed chow diet. All mice were housed, handled, and euthanized in accordance with NIH and institutional guidelines of The Ohio State University Institutional Animal Care and Use Committee.

DEN-Induced Primary Tumor Model

Liver tumors were induced in miR-122 LKO and floxed littermate (control) mice on a C57BL6 background by a single DEN injection (25 mg/kg body weight) on postnatal day 14 (P14), following published protocol,[18] and were sacrificed at specified time points post-DEN injection. Saline-injected mice were used as controls. Body weight, liver and tumor weights, and the tumor number were documented, and sera were collected.

Histological and Serological Analysis

H&E and Sirius Red staining of tissue sections were performed as described.[19] The scoring of inflammation and steatosis was performed on H&E-stained sections (×100 magnification) using the following criteria: 0, no inflammation; 1, mild lymphocytic infiltration in the portal triad; 2, severe lymphocytic infiltration in the portal triad; and 3, extended infiltration of lymphocytes throughout liver. Serology was performed as described.[15]

Immunohistochemistry

Formalin-fixed, paraffin-embedded sections were subjected to immunohistochemistry (IHC) for Ki-67, cytokeratin-19 (CK-19), α-fetoprotein (Afp), and bromodeoxyuridine (BrdU) incorporation as described.[15,18] The antibodies used for IHC were as follows: rabbit anti−Ki-67 (ab-15580; Abcam, Cambridge, MA); rabbit anti-CK19 (a generous gift from Dr. Joshua Freeman)[20]; mouse anti-Afp (AF5369; R&D Systems, Minneapolis, MN), and mouse anti-BrdU (B8434; Sigma-Aldrich, St. Louis, MO). Ki-67−positive cells were counted in five randomly selected fields at ×400 magnification, typically containing approximately 90 to 110 hepatocytes.

MRI

Magnetic resonance imaging (MRI) of liver tumors in mice was performed as described.[21]

Northern Blot Analysis and TaqMan Assay

Northern blot analysis and TaqMan (Life Technologies, Carlsbad, CA) assay of miR-122 were as described.[12]

Western Blot Analysis

Proteins were extracted from liver tissues in the lysis buffer containing protease and phosphatase inhibitor cocktails as described,[15] and 50 to 100 μg of proteins were subjected to Western blot analysis with specific antibodies. Catalog numbers and companies of antibodies used are provided as follows: from Santa Cruz Biotechnology (Dallas, TX): anti-Adam10 (sc-28358), anti-Afp (sc-8108), anti-Axl (sc-1096), anti-Ccng1 (sc-718), anti-Cdc25a (sc-7389), anti-E2f1 (sc-193), and anti-Srf (sc-335); from Millipore (Billerica, MA): anti-Gapdh (MAB374).

Real-Time RT-qPCR

Real-time quantitative RT-PCR (RT-qPCR) analysis of mRNAs was performed using SYBR Green chemistry (Life Technologies). Relative expression was calculated using the $\Delta\Delta C_T$ method.[22] The primer sequences are provided in Table 1.

3′-Untranslated Region Cloning and Luciferase Reporter Assay

3′-Untranslated regions (UTRs) of *Axl* and *Cdc25a* spanning miR-122 cognate sites were amplified from genomic DNA using specific primers and were cloned into psiCHECK2 vector. Transfection of the reporter with miR-122 mimic or negative control RNA and luciferase assays were performed as described.[15] The primer sequences are provided as follows: Axl-3′-UTR XhoI forward, 5′-CCGCTCGAGTGAGACA-ATCTTCCACCTGGGAC-3′; Axl-3′-UTR NotI reverse, 5′-ATAAGAATGCGGCCGCGGTGTCCAGCATTAGAAGT-GGTTAG-3′; Axl del 3′-UTR XhoI forward, 5′-CCGCTCG-AGACATCTTCCATCCCAGCGTTC-3′; Cdc25a-3′-UTR XhoI forward, 5′-CCGCTCGAGAAGACCTAAAGAAGT-TCCGCAC-3′; Cdc25a-3′UTR NotI reverse, 5′-AAGAATG-CGGCCGCTGCCCACCCAACACTGATTG-3′; Cdc25a-del 3′-UTR XhoI forward, 5′-CCGCTCGAGCCGTTACACT-CTTCTGTTCTG-3′.

Transfection of E2f1 siRNA

Hepa cells cultured in Dulbecco's modified Eagle's medium containing 10% fetal bovine serum were transfected with 60 nmol/L E2f1 siRNA (M-044993-03) or negative control siRNA (D-001206-13-05) obtained from Thermo Fisher Scientific (Waltham, MA) using Lipofectamine 2000 (Invitrogen, Grand Island, NY) for 4 hours. The expression of E2f1 and Cdc25a at RNA and protein levels were measured 48 hours post-transfection.

Dihydroethidine Staining

For assessing superoxide anions, frozen optimal cutting temperature compound embedded liver sections were incubated with 10 μmol/L dihydroethidine (DHE) (Sigma-Aldrich) at 37°C for 30 minutes and counter stained with DAPI (Santa Cruz Biotechnology, Dallas, TX).[21] The red fluorescence of DHE oxidized by superoxide anions and blue fluorescence of DAPI-stained nuclei were detected by an Olympus FV1000 Filter confocal microscope (Olympus, Center Valley, PA).

Statistical Analysis

Real-time RT-qPCR analysis was performed in triplicate. The data were presented as means ± SD. Most of the experiments were repeated twice. Statistical significance was calculated with the Student *t*-test, with a P value of <0.05 considered significant.

Table 1 Primers for Real-Time RT-qPCR

Name	Sequence
IL6 RTForward	5′-AGACTTCACAGAGGATACCACTCCC-3′
IL6 RTReverse	5′-TCTCATTTCCACGATTTCCCAG-3′
Tnfa RTForward	5′-ACCGTCAGCCGATTTGCTATC-3′
Tnfa RTReverse	5′-TCAGAGTAAAGGGGTCAGAGTGGG-3′
IL1b RTForward	5′-AAAAAAGCCTCGTGCTGTCG-3′
IL1b RTReverse	5′-GTCGTTGCTTGGTTCTCCTTG-3′
mAxl RTForward	5′-CATTGCCAAGATGCCAGTCAAG-3′
mAxl RTReverse	5′-CCACATTGTCACACCGAAGGAC-3′
hAxl RTForward	5′-ACCTTCAACTCCTGCCTTCTCG-3′
hAxl RTReverse	5′-TAACGGGTCTCCTTCTTTCGCC-3′
Gapdh RTForward	5′-TCCTGCACCACCAACTGCTTAG-3′
Gapdh RTReverse	5′-TGCTTCACCACCTTCTTGATGTC-3′
Cdc25a RTForward	5′-ATGGCTTCATAGACCTTCTGGATG-3′
Cdc25a RTReverse	5′-TGGGCACACTCTTCCTCCTCTTTG-3′
Cdc25a hnRNA RTForward	5′-CACGGGGAAGATGCTGTTTG-3′
Cdc25a hnRNA RTReverse	5′-TCTGTTTCCTGCTGGATCATCC-3′
E2f1 RTForward	5′-TGACGGTGTCGTTGACCTGAAC-3′
E2f1 RTReverse	5′-CTTGGACTTCTTGGCAATGAGC-3′
c-Jun RTForward	5′-TGGGCACATCACCACTACACC-3′
c-Jun RTReverse	5′-GGTTGAAGTTGCTGAGGTTGGC-3′
Adam10 RTForward	5′-GCTGGGAGGTCAGTATGGAAATC-3′
Adam10 RTReverse	5′-TGGCACGCTGGTGTTTTTGG-3′
Epcam RTForward	5′-GATGAAAAGGCACCCGAGTTC-3′
Epcam RTReverse	5′-TAACCAGGACAACAATCCCCGC-3′
Ctnnb1 RTForward	5′-GCTGGTGAAAATGCTTGGGTC-3′
Ctnnb1 RTReverse	5′-GCTTGCTCTCTTGATTGCCATAAG-3′
Igf2 RTForward	5′-CCTGGAGACATACTGTGCCACC-3′
Igf2 RTReverse	5′-TTGGAAGAACTTGCCCACGG-3′
Mapkapk2 RTForward	5′-CATCACCGACGACTACAAGGTCAC-3′
Mapkapk2 RTReverse	5′-GACAATCAGCAGGCACTTCCTC-3′
Ndrg3 RTForward	5′-GGCTTACCAAAAGGAAACAGACC-3′
Ndrg3 RTReverse	5′-GTGAGAACAGGAGGCAGCATC-3′
Tgfb RTForward	5′-CCAACTATTGCTTCAGCTCC-3′
Tgfb RTReverse	5′-GGTCCAGGCTCCAAAT-3′
Vegf RTForward	5′-GATCATGCGGATCAAACCTCACC-3′
Vegf RTReverse	5′-TTTACACGTCTGCGGATCTTGGAC-3′
Vimentin RTForward	5′-GATGTTGACAATGCTTCTCTGGC-3′
Vimentin RTReverse	5′-ATGCTGTTCCTGAATCTGGGC-3′
Ctgf RTForward	5′-CACCAGTGTGAAGACATACAGGGC-3′
Ctgf RTReverse	5′-TCGGGGCATTTGAACTCCAC-3′

Results

Early Onset of Hepatobiliary Cysts at Preneoplastic Stage in miR-122 LKO Mice on Exposure to DEN

To examine the pathological consequence of miR-122 loss on challenge with a hepatocarcinogen DEN, we used recently characterized LKO mice harboring liver-specific miR-122 ablation.[15] LKO and littermate control mice were injected with a single dose of DEN at P14 when it acts as a complete carcinogen.[18] Real-time RT-qPCR RT-qPCR analysis showed that the hepatic miR-122 level was barely detectable (approximately 0.7% of the wild-type level) at this age (Supplemental Figure S1A).

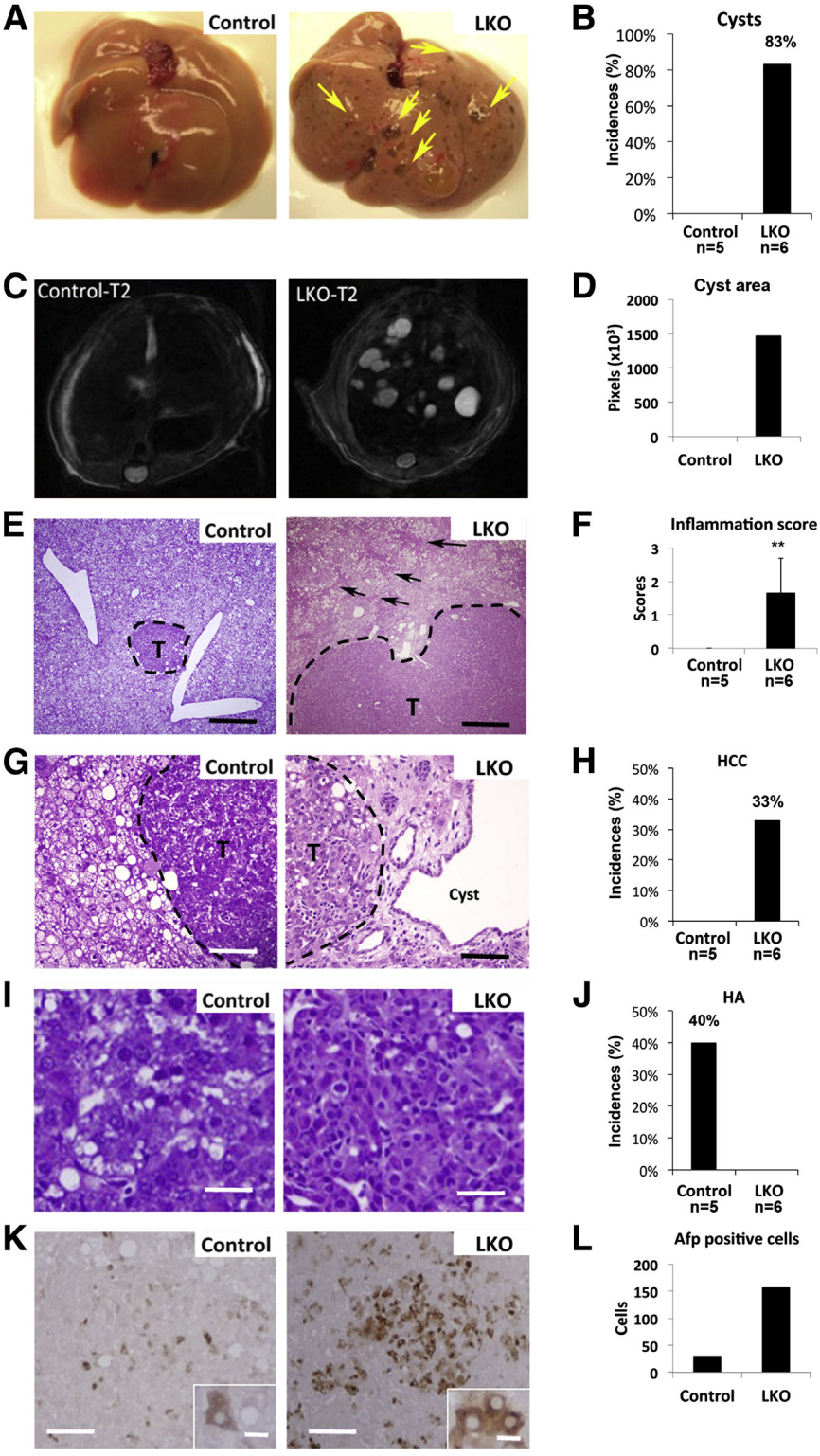

Figure 1 Diethylnitrosamine (DEN)-treated liver-specific miR-122 knockout (LKO) mice developed liver cysts and hepatocellular carcinoma (HCC)-like nodule at week 25 post-DEN exposure. **A:** Representative images of the livers from DEN-injected control (floxed) and miR-122 LKO mice exhibited appearance of cysts only in LKO mice. **B:** The incidence of cysts developed in control (n = 5) and LKO (n = 6) mice. **C:** T2-weighted MRI of liver in control and LKO mice with transverse section. **Arrows** denote cysts. **D:** Quantification of cyst area. **E**, **G**, and **I:** H&E staining of microscopic tumor (T) and surrounding liver tissues from DEN-injected control and LKO mice. **F:** The inflammation index of liver tissues from DEN-injected control (n = 5) and LKO (n = 6) mice. The scoring method is described in *Materials and Methods*. **H** and **J:** The incidences of HCC (**H**) and hepatocellular adenoma (HA) (**J**) developed in control (n = 5) and LKO (n = 6) mice. **K:** IHC with Afp antibody showed that the tumor in LKO mice is predominantly Afp positive. **L:** Quantification of the number of Afp-positive cells. Original magnification: ×100 (**E**), ×200 (**G**), and ×400 (**I**). Scale bars: 400 μm (**E**); 80 μm (**G** and **L**); 20 μm (**I**); and 10 μm (**K**, **inset**). $^{**}P \leq 0.01$.

Five DEN-injected mice of each genotype were sacrificed and analyzed at week 25 post-DEN treatment when dysplastic nodules are typically formed.[23] Notably, LKO mice developed macroscopic cysts in 83% of liver lobes, which were not visible in DEN-exposed control mice (Figure 1, A, B and D). Intrahepatic cysts, visualized as bright spots by T2-weighted MRI, were only detected in LKO mice (Figure 1C). H&E staining showed that both LKO and control mice developed steatosis, whereas hepatitis was developed only in LKO mice (Figure 1, E and F). Microscopic tumors were developed in both genotypes. However, LKO mice predominantly developed Afp-positive HCC (Figure 1, G, I, and K; Figure 1H shows the incidences of HCC), whereas control mice only developed hepatocellular adenoma (HA) (Figure 1, G, I, and K; Figure 1J shows the incidences of HA). HA and HCC were characterized based on the established morphological criteria, including existence of trabecular growth pattern of cancer cells, vascular invasion of tissues, malignancy of proliferating cells, expression of α-fetal protein.[24,25] Saline-injected LKO, but not control, mice developed microsteatosis and hepatitis at 25 weeks, but none developed tumors (data not shown). Up-regulation of several protumorigenic factors such as *c-Jun*, *Ctnnb1*, and several miR-122 targets, eg, *Adam10*, *Ndrg3*, and *Mapkapk2* in DEN-injected livers compared to controls (Figure 2A) correlated with increased susceptibility of LKO mice to form dysplastic foci. Many of these genes were also up-regulated or not changed in untreated LKO livers compared to control livers (Supplemental Figure S1D) and were further elevated in DEN exposed livers.

The microscopic tumors developed in DEN-treated LKO mice were more proliferative than those in control mice as demonstrated by fivefold more Ki-67−positive cells (a representative image is shown in Figure 2B). Moreover, IHC analysis with anti-CD34 antibody revealed abundance of vascular endothelial cells, both in the tumor and benign liver tissues of LKO mice, compared to that in control mice at 25 weeks post-DEN injection (Figure 2, C and D). Notably, more CD34-positive cells accumulated in the portal area of LKO mice compared to controls (Figure 2D). Sirius red staining showed that DEN-injected LKO livers exhibited severe fibrosis compared to control mice (Figure 2E). Increased expression of insulin-like growth factor 2 (Igf2), vascular endothelial growth factor-α (Vegf-α), and Vimentin correlated with pronounced angiogenesis in LKO livers, whereas up-regulation of Ctgf correlated with enhanced fibrosis in LKO livers (Figure 2, A and F). Notably, the expression of hepatic Vimentin and Ctgf (Supplemental Figure S1D) were elevated in saline-injected LKO mice

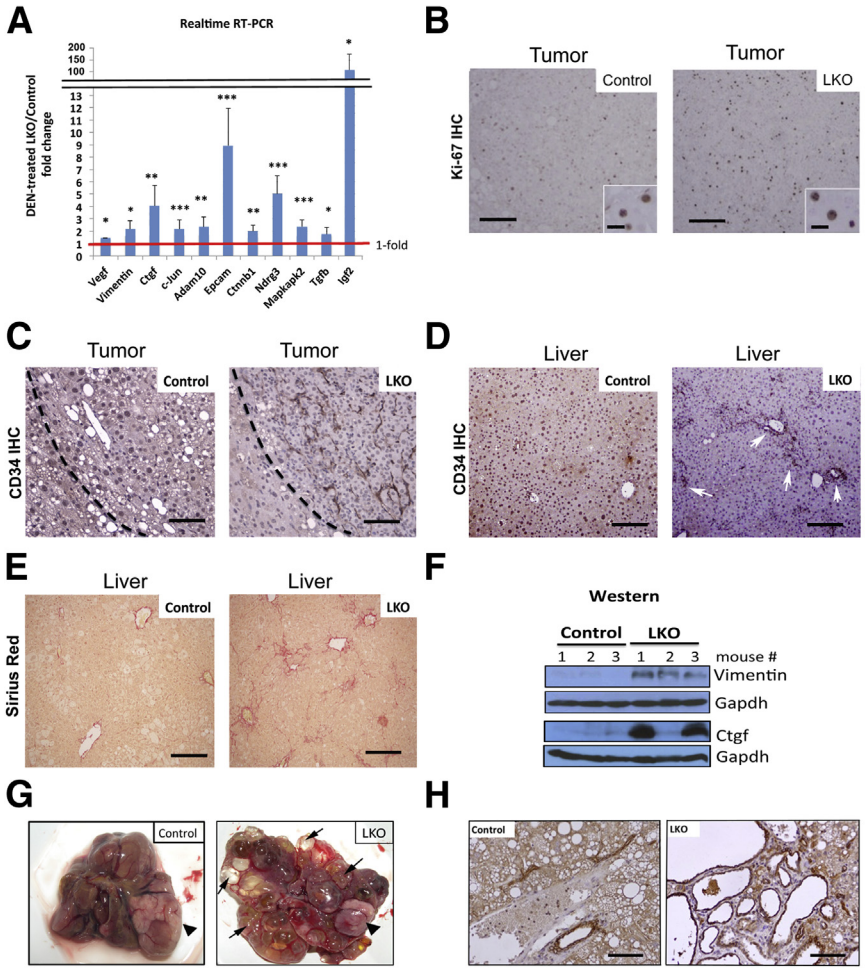

Figure 2 LKO mice exhibited more proliferative, vascular, and fibrotic livers at 25 weeks following diethylnitrosamine (DEN) treatment. **A:** Real-time RT-qPCR analysis (SYBR Green assay) of several tumor-promoting genes, including miR-122 targets, in control and LKO livers at 25 weeks post-DEN injection. Relative expression of indicated proteins in DEN-injected control livers was arbitrarily set at one. **B:** Ki-67 IHC revealed that microscopic tumors in LKO mice are more proliferative than the controls. **C** and **D:** IHC of liver tumor (**C**) and normal matching liver (**D**) with CD34 antibody. CD34-positive cells were more abundant in the tumor and livers of LKO mice compared to those in control mice. **Arrows** indicate CD34-positive cells in portal area, which are stained dark brown. **E:** LKO livers developed more fibrosis on DEN exposure compared to controls as demonstrated by Sirius red staining of fibrotic tissues. **F:** Western blot analysis of Ctgf, Vimentin, and Gapdh in liver extracts of mice at 25 weeks post-DEN injection and saline injection. **G:** Representative images of control and LKO liver covered with multiple cysts (**arrows**) and tumors (**arrowhead**) at week 44 following DEN injection. **H:** Representative images of CK19 IHC of liver section of control and LKO mice bearing cysts at week 25 post-DEN injections. Cells stained dark brown are CK-19−positive cells. Scale bars: 80 μm (**B**); 25 μm (**B**, inset); 50 μm (**C**); 100 μm (**D** and **E**).

and increased further on DEN exposure (Figure 2A). Taken together, these results indicate that hepatic loss of miR-122 promoted angiogenesis, and fibrosis at the pre/neoplastic stage after single DEN exposure at the postnatal stage.

Hepatic *Cdc25a*, which Promotes Cystogenesis, Is Up-Regulated in miR-122 LKO Mice on DEN Exposure

Formation of cysts at the preneoplastic stage only in DEN-treated LKO mice and their dramatic spread in all liver lobes with time (Figure 2G) suggested for us to characterize these cysts. IHC analysis showed that these liver cysts were lined with CK19-positive cholangiocytes (Figure 2H). We focused our attention to *Cdc25a* because it has recently been shown to play a causal role in hepatobiliary cyst formation by inducing the proliferation of cystic cholangiocytes.[26] Indeed, both RNA and protein levels of Cdc25a increased more than twofold in DEN-injected LKO mice compared to control mice (Figure 3, A and B).

Next, we sought to understand the mechanism of up-regulation of *Cdc25a* in DEN-injected LKO mice. First, we measured miR-15a, because its down-regulation is reported to contribute to hepatic cystogenesis by up-regulating *Cdc25a*.[27] However, expression of miR-15a and miR-16 that can target *Cdc25a* was not significantly altered in LKO livers compared to controls (Supplemental Figure S1B).

Because TargetScan[28] predicted *Cdc25a* as a potential miR-122 target (Figure 3A), we performed a luciferase assay after cloning the *Cdc25a* 3′-UTR into psiCHECK2 vector. However, miR-122 did not affect reporter activity driven by *Cdc25a* 3′-UTR (Figure 3A), suggesting that it is not a direct target of miR-122. Moreover, real-time RT-qPCR (Figure 3B) and Western blot (data not shown) analyses did not show up-regulation of *Cdc25a* in saline-injected LKO livers, suggesting that DEN exposure indirectly activated the *Cdc25a* gene in these mice. Indeed, real-time RT-qPCR analysis confirmed up-regulation of *Cdc25a* primary transcript (hnRNA) and mRNA at comparable levels (approximately two- to threefold) at preneoplastic stage in LKO livers (Figure 3B), indicating its transcriptional induction.

We then attempted to elucidate the mechanism of induction of *Cdc25a* in DEN-exposed LKO livers. E2f1, an important cell-cycle regulator, has been reported to activate the *Cdc25a* gene.[29] We hypothesized that up-regulation of E2f1 in DEN-treated LKO livers might play a causal role in the induction of *Cdc25a,* thereby promoting cyst formation. Indeed, E2f1 was up-regulated in DEN-exposed LKO livers at the preneoplastic stage (Figure 3, C and D), and siRNA-mediated knockdown of E2f1 reduced the *Cdc25a* level both at the mRNA (25%) and protein levels (40%) in Hepa cells (Figure 3, E and F). Notably, siRNA-mediated knockdown of E2f1 protein level (80%) was more pronounced than its RNA level (40%). Taken together, these results suggest that E2f1-mediated activation of *Cdc25a* is one of the mechanisms involved in cystogenesis in LKO mice on DEN exposure.

DEN-Induced Liver Damage and HCC Incidence Are Significantly Higher in LKO Mice

At week 35 following DEN injection, 14 mice of each genotype were sacrificed to assess tumor burden. Although the total number of macroscopic tumors developed in mice was

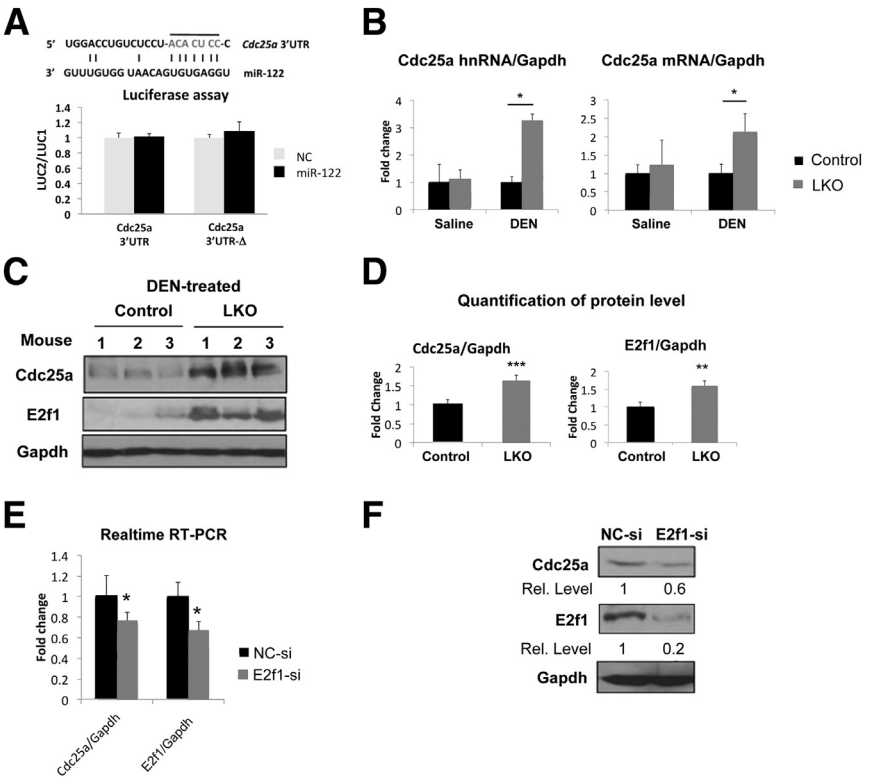

Figure 3 E2f1-mediated transcriptional induction of Cdc25a may induce liver cysts in LKO mice. **A**: Renilla luciferase activity (LUC2) produced from wild-type or mutant Cdc25a 3′-UTR reporter plasmids or empty vector normalized to firefly luciferase activity (LUC1) produced from the same plasmid after transfection into Hepa cells together with negative control (NC) RNA or miR-122 mimic. Error bars represent standard deviations derived from three independent experiments. **B**: Both pre-mRNA (hnRNA) and mRNA are up-regulated at similar level in DEN-injected LKO livers. Real-time RT-qPCR analysis of Cdc25a mRNA and hnRNA in livers ($n = 5$) was performed. The data were normalized to Gapdh RNA level. **C**: Western blot analysis of liver extracts with specific antibodies at week 25 post-DEN injection. **D**: Quantification of the protein signals. mRNA (**E**) and protein levels (**F**) of Cdc25a and E2f1 in Hepa cells transfected with 60 nmol/L negative control or E2f1 siRNA ($n = 3$). The results were normalized to Gapdh level. $^{*}P \leq 0.05$, $^{**}P \leq 0.01$, and $^{***}P \leq 0.001$.

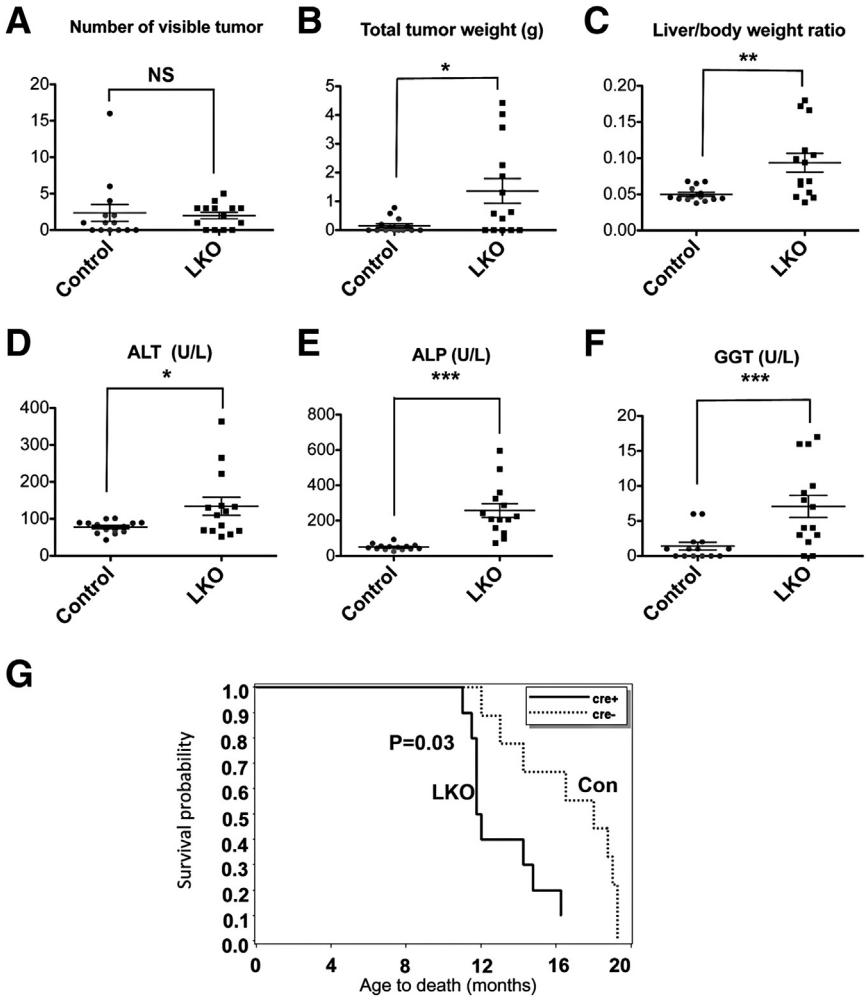

Figure 4 LKO mice exhibited higher tumor burden and hepatobiliary injury at week 35 post-diethylnitrosamine (DEN) injection. **A:** Number of macroscopic tumors developed in mice. **B:** Total weight of tumors harvested from DEN-injected mice. **C:** Liver/body weight ratio of DEN-injected mice. **D**–**F:** Serological analysis of DEN-injected mice. **G:** Survival curve of female LKO and control mice injected with 25 mg/kg DEN on P14. Because all mice died at the end of the study, the two-sample *t*-test was used to test the survival difference. The Kaplan-Meier survival curves were generated to display the results. $n = 9$ for control (cre−) mice and $n = 10$ for LKO (cre+) mice. ALT, alanine aminotransferase; ALP, alkaline phosphatase; GGT, gamma-glutamyltransferase.*$P \leq 0.05$, **$P \leq 0.01$, and ***$P \leq 0.001$.

not significantly different between the two genotypes (Figure 4A), the total tumor weight (approximately ninefold, $P = 0.015$) was higher in the mutant mice (Figure 4B), suggesting faster tumor growth in LKO mice. Twofold increase in liver to body weight ratios (Figure 4C) and elevated serum alanine aminotransferase (ALT) (approximately 1.7-fold), gamma-glutamyltransferase (GGT) (approximately fivefold) and alkaline phosphatase (ALP) (approximately fivefold) (Figure 4, D–F) levels indicated excessive liver damage in LKO mice compared to controls. Elevation of serum ALP is a characteristic of animals depleted of miR-122 by injecting locked nucleic acid–modified anti-sense oligonucleotides[30] or genetic ablation,[15,16] even without carcinogen exposure.

As shown in Figure 5A, LKO mice at week 35 post-DEN exposure developed larger tumor and numerous cysts, whereas control mice developed only smaller tumors. MRI of a few mice demonstrated bigger tumors and cysts in LKO mice compared to controls (a representative image is shown in Figure 5B). Histological analysis of H&E-stained sections demonstrated that 71% (10 of 14) of LKO mice developed HCC as opposed to only 21.4% (3 of 14) of control mice formed HCC (Figure 5, C and F). At 35 weeks, 86% (12 of 14) of LKO mice developed macroscopic liver cysts, as opposed to none in control mice (Figure 5, D and F). Analysis of the cystic fluid from a few mice showed high levels of ALT, GGT, ALP, and bile acids (data not shown). CK-19–positive cholangiocarcinoma was detected in two LKO mice (Figure 5, D and F). By contrast, the majority of liver tumors developed in control mice were hepatocellular adenoma (Figure 5C). BrdU incorporation, an index of proliferation, was approximately fourfold higher ($P = 0.03$) in tumors developed in LKO mice than those in control mice (Figure 5E). Metastatic lung tumors were detected only in three LKO mice (data not shown).

Almost all DEN-injected female LKO mice developed tumors and cysts with age and exhibited reduced survival compared with the control mice, as evident from the death of 6 of 10 LKO mice within 12 months of DEN injection, whereas all control mice were still alive (Figure 4G). The tumor weight, liver damage, and cyst formation were significantly higher in female LKO mice compared to controls (data not shown). Collectively, these results demonstrate that loss of miR-122 enhances susceptibility of mice to a liver carcinogen.

Up-Regulation of Several Oncogenic Targets of miR-122 Including Axl, a Receptor Tyrosine Kinase, Correlates with Enhanced Susceptibility of LKO Mice to Hepatocarcinogenesis on DEN Exposure

Previously, we have shown that loss of miR-122 induces up-regulation of genes involved in cell proliferation, including fetal genes in liver.[15] Several of these genes are confirmed as direct targets of miR-122.[12,31] To understand the role of these targets in promoting DEN-induced tumorigenesis, we measured their expression in tumors developed in control and LKO mice by immunoblotting. The results showed that three miR-122 targets *Adam10*, *Ccng1*, and *Srf* were significantly increased by approximately 2-, 2.5-, and 2-fold, respectively, in LKO tumors compared to controls (Figure 6, A and B). Elevation of *Afp* (threefold), a fetal gene and a marker of HCC, in all LKO tumors compared to those in controls correlated with the histopathological analysis (Figure 5, C and F). As expected, both *E2f1* and *Cdc25a* were also up-regulated in LKO tumors (Figure 6, A and B).

Axl, a receptor tyrosine kinase, is up-regulated in different neoplasms, including HCC, and exhibits characteristics of an oncogene.[32] It is also a predicted target of miR-122 in mouse (Figure 6C) and human (Table 2). Microarray analysis showed an approximately 1.8-fold ($P = 0.001$) up-regulation of Axl in LKO livers, which was confirmed by real-time RT-qPCR (Figure 6D) and Western blot analysis (Figure 6, E and F); we were curious to know whether Axl level was elevated in DEN-induced LKO tumors. Indeed, the Axl protein level increased 1.9-fold ($P = 0.0001$) in LKO tumors compared to controls (Figure 6, A and B).

We next investigated whether Axl is a true target of miR-122 by measuring Axl-3′-UTR–driven renilla luciferase. Relative luciferase activity (renilla to firefly) was reduced by

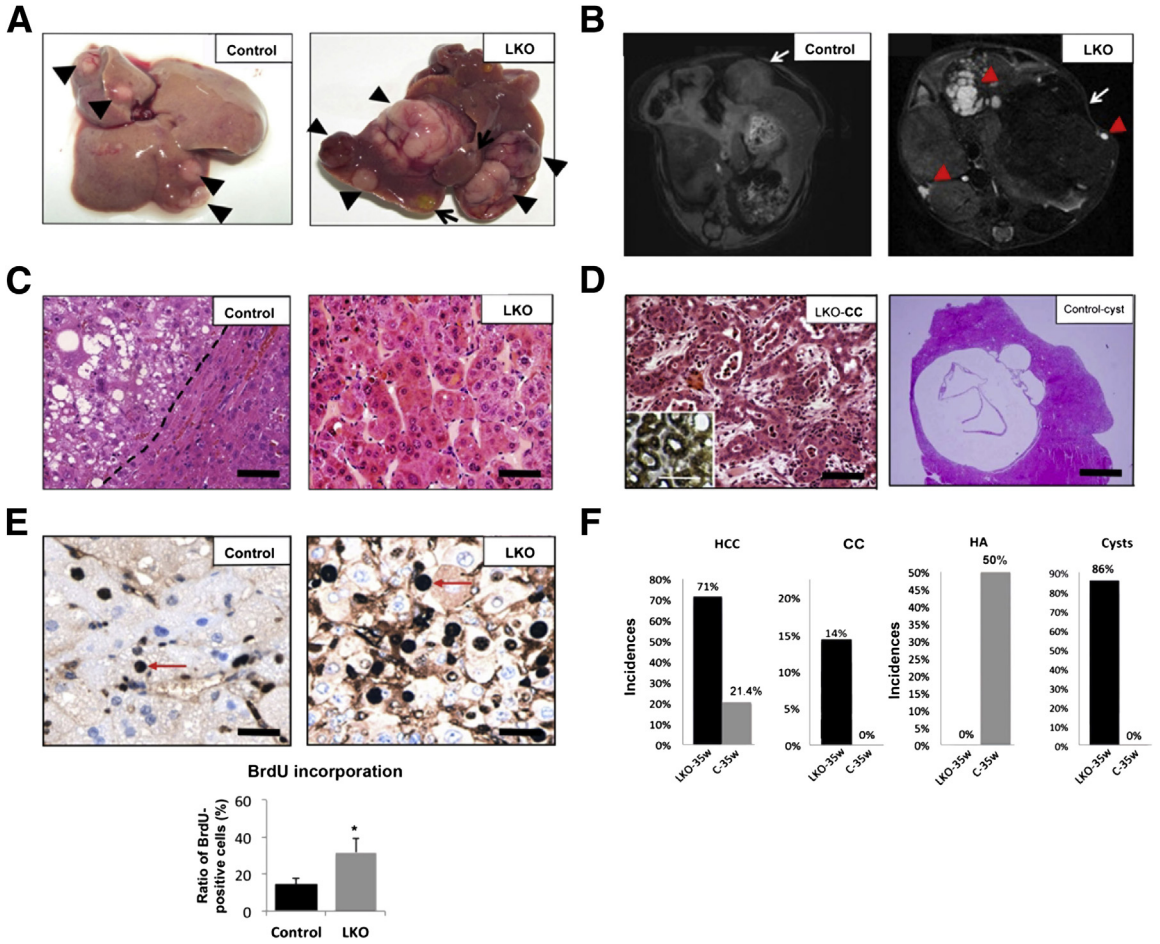

Figure 5 Loss of miR-122 in liver promoted hepatocellular carcinoma (HCC) and liver cysts at week 35 postdiethylnitrosamine (DEN) exposure. **A:** Representative images of livers showing bigger macroscopic tumors and cysts developed in LKO mice. **Arrows** indicate cysts; **arrowhead**, tumors. **B:** T2-weighted MRI image of liver with transverse section. **Arrowheads** indicate cysts; **arrows,** tumors. **C:** Representative H&E stained images of hepatocellular adenoma (HA) and HCC identified in control and LKO mice, respectively. **D:** H&E staining of cholangiocarcinoma (CC) and cysts identified in LKO mice. The **inset** represents CK-19–positive cholangiocytes. **E:** IHC of liver tumors with BrdU antibody in mice injected with BrdU 3 hours before euthanasia. **Arrows** indicate BrdU-positive cells. The BrdU-positive cells in control and LKO liver tumors were quantified and presented in the **right panel**. **F:** The incidence of indicated pathological features, including HCC, CC, HA, and cysts in livers harvested from DEN injected control ($n = 14$) and LKO ($n = 15$) mice at 35 weeks. Scale bars: 50 μm (**C**); 50 μm (**D**, **left panel**, **inset**); 500 μm (**D**, **right panel**); 20 μm (**E**).*$P \leq 0.05$.

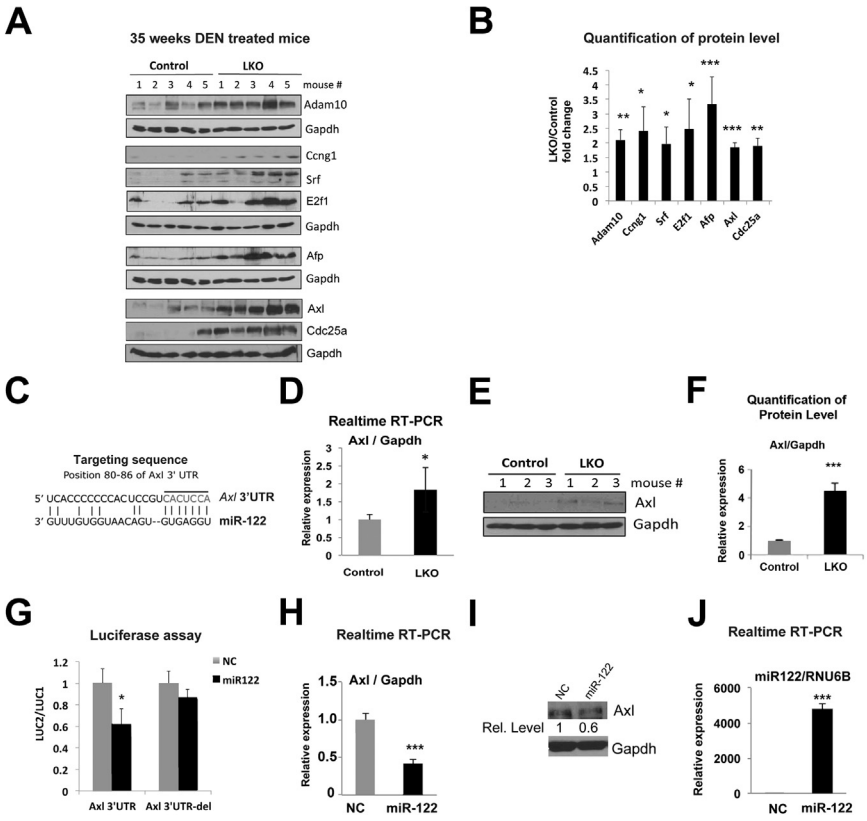

Figure 6 Up-regulation of genes involved in oncogenesis, including miR-122 targets, in tumors developed in LKO mice. **A**: Western blot analysis of indicated proteins in tumor extracts from control and LKO mice at week 35 postdiethylnitrosamine (DEN) injections. **B**: Quantitative representation of the Western blot data in **A**. The band intensity was quantified using ImageJ software version 1.46r (NIH, Bethesda, MD), and the data were normalized to Gapdh level. Fold increase in indicated proteins in LKO tumors compared to control tumors are presented. **C**: Predicted miR-122 binding site in the 3′-UTR of Axl. **D**–**F**: The hepatic expression of Axl in 10-week-old control and LKO mice was determined by real-time RT-qPCR (**D**) and Western blot analysis (**E** and **F**). **G**: Axl is a target of miR-122. Renilla luciferase activity (LUC2) produced from the wild-type or mutant Axl 3′-UTR reporter plasmids normalized to that of firefly luciferase (LUC1) after transfecting Hepa cells with the respective plasmid along with 25 nmol/L negative control RNA (NC) or miR-122 mimic. Error bars represent standard deviations derived from three independent experiments. mRNA (**H**) and protein (**I**) levels of Axl in Hep3B cells transfected with negative control RNA or miR-122 mimic. **J**: miR-122 level normalized to RNU6B was measured by real-time RT-qPCR ($n = 3$). $^{*}P \leq 0.05$, $^{**}P \leq 0.01$, and $^{***}P \leq 0.001$.

approximately 40% ($P = 0.007$) in cells cotransfected with the reporter (LUC-Axl 3′-UTR) and miR-122 compared to those transfected with negative control RNA, which was abrogated after deletion of the miR-122 cognate site from the reporter plasmid (LUC-Axl del 3′-UTR) (Figure 6G). Furthermore, ectopic miR-122 expression in Hep3B cells that do not express miR-122 reduced Axl mRNA expression both at the RNA (approximately 60%) and protein (approximately 40%) levels (Figure 6, H–J). Similar results were observed in Hepa cells (Supplemental Figure S2).

DEN Exposure Induces Oxidative Stress and Increases Expression of Proinflammatory Cytokines in miR-122 LKO Mice

DEN is enzymatically converted to reactive ethyldiazonium ion, which causes DNA damage by reacting with DNA bases. DEN is known to cause oxidative stress.[33] To examine whether LKO mice are sensitive to DEN-induced oxidative stress, we treated LKO mice with DEN and measured oxidative stress in frozen tissue sections by DHE staining, which reacts with superoxide anion. LKO livers exhibited more oxidative stress for 12 hours following DEN treatment, as demonstrated by the intense red fluorescence with DHE compared to controls (Supplemental Figure S3). Furthermore, much higher induction of IL6 (2.1-fold in control versus 11.8-fold in LKO), tumor necrosis factor-α (TNF-α) (3.8-fold in control versus 17.4-fold in LKO), and IL1β (1.4-fold in control versus 6.4-fold in LKO) in LKO livers exposed to DEN for 12 hours (Figure 7, A–C) occurred in mutant mice. Increased production of superoxide anion and induction of proinflammatory cytokines immediately after DEN injection suggest that LKO mice are more susceptible to genotoxic stress.

Discussion

Protective Role of miR-122 against a Chemical Carcinogen

miR-122 exhibits pleiotropic functions in mammals.[4] Although it is not essential for liver development, it is involved in lipid homeostasis and maintenance of hepatic function in adult mice.[15,16] However, it is still not clear how miR-122 deficiency may affect the development of liver tumor with the combination of other risk factors, such as chemical carcinogens. DEN is a carcinogen used frequently for induction of HCC in mice.[21] Here, we have demonstrated that loss of miR-122–expedited DEN-induced HCC development in mice. DEN-injected LKO mice exhibited larger tumor mass and higher incidence of HCC compared to DEN-injected control mice. Carcinogen-induced liver damage was also more pronounced in LKO mice. Notably, DEN exposure on P14 also caused liver tumor development in female LKO mice that were found to be resistant to spontaneous tumorigenesis.[15] However, unlike tumors

Table 2 RNA22 Algorithm Predicts Existence of Multiple miR-122 Complementary Sites in 3′-UTR of Both Spliced Variants of Human Axl mRNAs

Variant	Position	Predicted target site	Targeting miRNA sequence
#1 ENST00000359092			
hsa_miR_122	4152	5′-TTTCAAGGCACTCTAGATTCCA-3′	5′-TGGAGTGTGACAATGGTGTTTG-3′
hsa_miR_122	4089	5′-AGATTCTAGATCAGATGCTCCA-3′	5′-TGGAGTGTGACAATGGTGTTTG-3′
hsa_miR_122	2893	5′-ACTGCCACTGGGGAAAACTCCA-3′	5′-TGGAGTGTGACAATGGTGTTTG-3′
#2 ENST00000301178			
hsa_miR_122	4179	5′-TTTCAAGGCACTCTAGATTCCA-3′	5′-TGGAGTGTGACAATGGTGTTTG-3′
hsa_miR_122	4116	5′-AGATTCTAGATCAGATGCTCCA-3′	5′-TGGAGTGTGACAATGGTGTTTG-3′
hsa_miR_122	2920	5′-ACTGCCACTGGGGAAAACTCCA-3′	5′-TGGAGTGTGACAATGGTGTTTG-3′

developed in liver-specific *Ctnnb1* knockout mice,[34] those produced in LKO mice were not significantly repopulated with miR-122–positive hepatocytes that escaped Cre-mediated deletion (Supplemental Figure S1C). Interestingly, DEN exposure caused liver cyst formation only in LKO mice, irrespective of the sex. Cysts do not commonly occur in human HCC patients, unless there is internal necrosis caused by certain therapies such as radiofrequency ablation.[35] To the best of our knowledge, there is no report about the cyst formation induced just by a single DEN injection in mice, except in a few cases with continuous treatment of DEN at high doses for several weeks[36] or in combination with pentachlorophenol.[37] The present study is the first to observe the significant effect of miR-122 deficiency on hepatic cyst formation.

One crucial factor in hepatocarcinogenesis is chronic hepatic inflammation,[38] which is induced by the loss of miR-122 and is exhibited in the liver of DEN-treated LKO mice. We have shown that the activation of the Ccl2–Ccr2 axis plays a causal role in hepatic inflammation in these mice.[15] However, we cannot rule out the involvement of additional mechanisms, such as hypoxia, which is known to induce sterile inflammation through the activation of proinflammatory gene programs, such as TLR-induced NF-κB signaling and chemokine secretion (reviewed in[39]). Simultaneously, certain hypoxia-induced genes, such as *HIF*, can protect cells from injury by inhibition of apoptosis or induction of adenosine signaling.[40,41] Therefore, it will be intriguing to see whether hypoxia can regulate hepatic inflammation through its transcriptional regulation of miR-122. Previously, it was reported that miR-122 was down-regulated by hypoxia,[42] which implies a possibility that the miR-122 deficiency–induced inflammation could be a result of hypoxia.

The Role of *Cdc25a* in Cyst Formation

To explore the mechanism of DEN-induced cyst development in LKO mice, we looked for potential target genes that are known to be involved in cystogenesis in liver. *Cdc25a* is one such candidate gene that has recently been shown to play a pivotal role in hepatic and renal cyst formation in rodent models.[37] Interestingly, Cdc25a was up-regulated in DEN injected LKO mice compared to the controls. However, expression miR-15a that targets Cdc25a and affects hepatic cystogenesis in polycystic kidney disease[27,43] remained unaltered in cyst-bearing LKO mice compared to DEN-injected control mice (data not shown). Prediction of Cdc25a as a direct target of miR-122 by TargetScan[28] led us to hypothesize that miR-122 deficiency resulted in activation of the *Cdc25a* gene in LKO mice. However, the inability of luciferase assay to confirm *Cdc25a* as a direct target of miR-122 and up-regulation of its primary transcript suggested transcriptional activation of *Cdc25a* in LKO mice at week 25

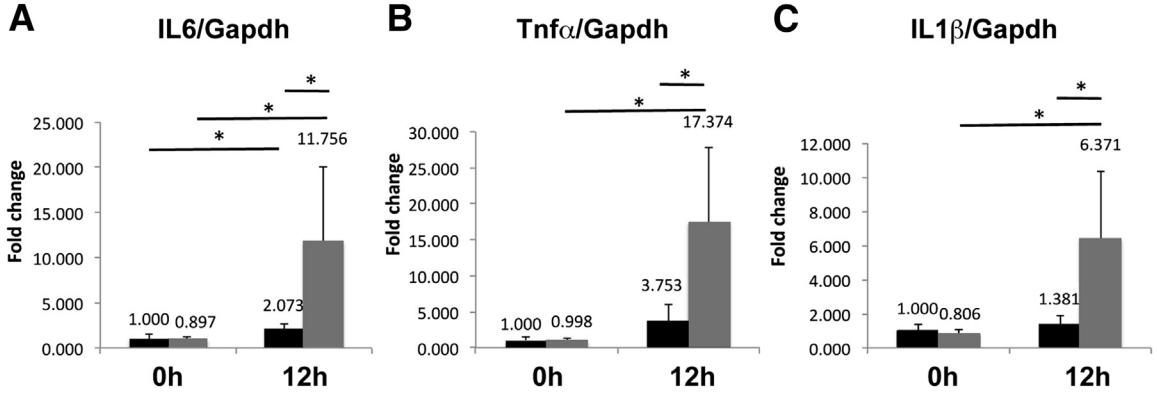

Figure 7 Postnatal dihydroethidine (DHE) exposure promoted oxidative stress and induced proinflammatory cytokines in LKO livers. **A**–**C**: mRNA levels of IL-6, TNF-α, and IL-1β were determined by real-time RT-qPCR in livers of control and LKO mice. The respective levels in saline injected controls were assigned a value of 1. $^*P \leq 0.05$.

post-DEN injection. We focused on E2f1, a known activator of the *Cdc25a* gene. Indeed, E2f1 was significantly elevated in DEN-exposed LKO livers, and siRNA-mediated depletion of E2f1 reduced the Cdc25a level in hepatic cells. Our data showed that DEN-induced oxidative stress is higher in LKO mice (Supplemental Figure S3) and may result in liver injury and compensatory proliferation of damaged hepatocytes, which is significantly higher in these mice compared to the control mice due to the activation of several growth promoters, including Igf2 (Figure 2A) and c-Myc.[15] E2f1, a cell-cycle promoter, is up-regulated in these proliferating cells, thereby increasing expression of Cdc25a. Therefore, it is likely that Cdc25a is one of the factors that contribute to cyst formation in LKO mice. However, we cannot rule out the involvement of additional factor(s) that might contribute to cystogenesis. Indeed, expression of two genes, *Sec63* and *Pkrcsh* that encode hepatocystin, are down-regulated in LKO livers (data not shown). Loss of expression of these genes due to germline or somatic mutation is associated with polycystic liver disease in humans, characterized by multiple fluid-filled cysts in the liver,[44,45] as observed in LKO mice exposed to DEN.

The Role of Axl, a Novel Target of miR-122, in Oncogenesis

Identification of Axl, a receptor tyrosine kinase, as a target of miR-122 merits discussion. Axl was first identified in patients with chronic myelogenous leukemia,[46] and correlation between its overexpression, metastasis, and poor prognosis was subsequently reported in different malignancies.[47] Axl is a downstream target of several key signaling pathways, eg, Tgf-β1, Hippo, and Vegf-A, and promotes oncogenesis by facilitating proliferation, migration, invasion, and angiogenesis and inhibiting apoptosis. Abundance of miR-122 is likely to be responsible for the suppression of Axl in the liver, and its up-regulation in tumors might play a causal role in producing highly invasive tumors in LKO mice. Interestingly, Axl is also elevated in tumors developed spontaneously in miR-122–deficient livers; Gene Expression Omnibus (*http://www.ncbi.nlm.nih.gov/geo*, accession number GSE31731). It would be of interest to investigate whether small molecule inhibitors of Axl can impede tumor growth in LKO mice. So far, studies from several laboratories, including ours, identified several tumor-promoting genes as direct targets of miR-122, including *Ccng1*, *Axl*, *Adam10*, and *Srf*. Among these genes, *Axl* and *Adam10* were both critical in the tumor migration and invasion, whereas *Ccng1* and *Srf* were both involved in proliferation of tumor cells. Through de-repression of these genes, loss of miR-122 in liver may promote a subset of hepatocytes to proliferate more aggressively than those in control mice during compensatory proliferation after liver damage induced by genotoxic chemicals such as DEN. On the basis of our results, we propose a model (Supplemental Figure S4) describing the consequence of miR-122 loss in DEN-induced liver pathogenesis.

In conclusion, our data show a novel function of miR-122 in suppressing DEN induced cystogenesis and HCC. These results further extend our knowledge about the protective role of miR-122 in the liver from genotoxic carcinogens. In the future, it would be of interest to examine whether inhibitors of *Cdc25a* and *Axl* can reverse the deleterious effect of the carcinogen.

Acknowledgments

We thank Dr. Samson Jacob for critically reading the manuscript, Dr. Joshua Friedman for providing CK-19 antibody, the Nucleic Acid Shared Resource and Small Animal Imaging Core facilities at the Ohio State University Comprehensive Cancer Center, and Thomas Kaffenberger, Vivek Chaudhuri, and Kun-yu Teng for technical assistance.

Supplemental Data

Supplemental material for this article can be found at *http://dx.doi.org/10.1016/j.ajpath.2013.08.004*.

References

1. Jemal A, Bray F, Center MM, Ferlay J, Ward E, Forman D: Global cancer statistics. CA Cancer J Clin 2011, 61:69–90
2. Altekruse SF, McGlynn KA, Reichman ME: Hepatocellular carcinoma incidence, mortality, and survival trends in the United States from 1975 to 2005. J Clin Oncol 2009, 27:1485–1491
3. El-Serag HB: Hepatocellular carcinoma. N Engl J Med 2011, 365: 1118–1127
4. Jopling C: Liver-specific microRNA-122: biogenesis and function. RNA Biol 2012, 9:137–142
5. Coulouarn C, Factor VM, Andersen JB, Durkin ME, Thorgeirsson SS: Loss of miR-122 expression in liver cancer correlates with suppression of the hepatic phenotype and gain of metastatic properties. Oncogene 2009, 28:3526–3536
6. Xu H, He JH, Xiao ZD, Zhang QQ, Chen YQ, Zhou H, Qu LH: Liver-enriched transcription factors regulate microRNA-122 that targets CUTL1 during liver development. Hepatology 2010, 52:1431–1442
7. Laudadio I, Manfroid I, Achouri Y, Schmidt D, Wilson MD, Cordi S, Thorrez L, Knoops L, Jacquemin P, Schuit F, Pierreux CE, Odom DT, Peers B, Lemaigre FP: A feedback loop between the liver-enriched transcription factor network and miR-122 controls hepatocyte differentiation. Gastroenterology 2012, 142:119–129
8. Gatfield D, Le Martelot G, Vejnar CE, Gerlach D, Schaad O, Fleury-Olela F, Ruskeepaa AL, Oresic M, Esau CC, Zdobnov EM, Schibler U: Integration of microRNA miR-122 in hepatic circadian gene expression. Genes Dev 2009, 23:1313–1326
9. Burns DM, D'Ambrogio A, Nottrott S, Richter JD: CPEB and two poly(A) polymerases control miR-122 stability and p53 mRNA translation. Nature 2011, 473:105–108
10. Krutzfeldt J, Rajewsky N, Braich R, Rajeev KG, Tuschl T, Manoharan M, Stoffel M: Silencing of microRNAs in vivo with 'antagomirs'. Nature 2005, 438:685–689
11. Kutay H, Bai S, Datta J, Motiwala T, Pogribny I, Frankel W, Jacob ST, Ghoshal K: Downregulation of miR-122 in the rodent and human hepatocellular carcinomas. J Cell Biochem 2006, 99:671–678
12. Bai S, Nasser MW, Wang B, Hsu SH, Datta J, Kutay H, Yadav A, Nuovo G, Kumar P, Ghoshal K: MicroRNA-122 inhibits tumorigenic

properties of hepatocellular carcinoma cells and sensitizes these cells to sorafenib. J Biol Chem 2009, 284:32015–32027
13. Tsai WC, Hsu PW, Lai TC, Chau GY, Lin CW, Chen CM, Lin CD, Liao YL, Wang JL, Chau YP, Hsu MT, Hsiao M, Huang HD, Tsou AP: MicroRNA-122, a tumor suppressor microRNA that regulates intrahepatic metastasis of hepatocellular carcinoma. Hepatology 2009, 49:1571–1582
14. Castoldi M, Vujic Spasic M, Altamura S, Elmen J, Lindow M, Kiss J, Stolte J, Sparla R, D'Alessandro LA, Klingmuller U, Fleming RE, Longerich T, Grone HJ, Benes V, Kauppinen S, Hentze MW: Muckenthaler MU: The liver-specific microRNA miR-122 controls systemic iron homeostasis in mice. J Clin Invest 2011, 121:1386–1396
15. Hsu SH, Wang B, Kota J, Yu J, Costinean S, Kutay H, Yu L, Bai S, La Perle K, Chivukula RR, Mao H, Wei M, Clark KR, Mendell JR, Caligiuri MA, Jacob ST, Mendell JT, Ghoshal K: Essential metabolic, anti-inflammatory, and anti-tumorigenic functions of miR-122 in liver. J Clin Invest 2012, 122:2871–2883
16. Tsai WC, Hsu SD, Hsu CS, Lai TC, Chen SJ, Shen R, Huang Y, Chen HC, Lee CH, Tsai TF, Hsu MT, Wu JC, Huang HD, Shiao MS, Hsiao M, Tsou AP: MicroRNA-122 plays a critical role in liver homeostasis and hepatocarcinogenesis. J Clin Invest 2012, 122:2884–2897
17. Hsu SH, Yu B, Wang X, Lu Y, Schmidt CR, Lee RJ, Lee LJ, Jacob ST, Ghoshal K: Cationic lipid nanoparticles for therapeutic delivery of siRNA and miRNA to murine liver tumor. Nanomedicine 2013, 9:1169–1180
18. Maeda S, Kamata H, Luo JL, Leffert H, Karin M: IKKbeta couples hepatocyte death to cytokine-driven compensatory proliferation that promotes chemical hepatocarcinogenesis. Cell 2005, 121:977–990
19. Wang B, Majumder S, Nuovo G, Kutay H, Volinia S, Patel T, Schmittgen TD, Croce C, Ghoshal K, Jacob ST: Role of microRNA-155 at early stages of hepatocarcinogenesis induced by choline-deficient and amino acid-defined diet in C57BL/6 mice. Hepatology 2009, 50:1152–1161
20. Hand NJ, Master ZR, Le Lay J, Friedman JR: Hepatic function is preserved in the absence of mature microRNAs. Hepatology 2009, 49:618–626
21. Majumder S, Roy S, Kaffenberger T, Wang B, Costinean S, Frankel W, Bratasz A, Kuppusamy P, Hai T, Ghoshal K, Jacob ST: Loss of metallothionein predisposes mice to diethylnitrosamine-induced hepatocarcinogenesis by activating NF-kappaB target genes. Cancer Res 2010, 70:10265–10276
22. Wang B, Hsu SH, Majumder S, Kutay H, Huang W, Jacob ST, Ghoshal K: TGFbeta-mediated upregulation of hepatic miR-181b promotes hepatocarcinogenesis by targeting TIMP3. Oncogene 2010, 29:1787–1797
23. Kalinichenko VV, Major ML, Wang X, Petrovic V, Kuechle J, Yoder HM, Dennewitz MB, Shin B, Datta A, Raychaudhuri P, Costa RH: Foxm1b transcription factor is essential for development of hepatocellular carcinomas and is negatively regulated by the p19ARF tumor suppressor. Genes Dev 2004, 18:830–850
24. Thoolen B, Ten Kate FJ, van Diest PJ, Malarkey DE, Elmore SA, Maronpot RR: Comparative histomorphological review of rat and human hepatocellular proliferative lesions. J Toxicol Pathol 2012, 25:189–199
25. Thoolen B, Maronpot RR, Harada T, Nyska A, Rousseaux C, Nolte T, Malarkey DE, Kaufmann W, Kuttler K, Deschl U, Nakae D, Gregson R, Vinlove MP, Brix AE, Singh B, Belpoggi F, Ward JM: Proliferative and nonproliferative lesions of the rat and mouse hepatobiliary system. Toxicol Pathol 2010, 38:5S–81S
26. Masyuk TV, Radtke BN, Stroope AJ, Banales JM, Masyuk AI, Gradilone SA, Gajdos GB, Chandok N, Bakeberg JL, Ward CJ, Ritman EL, Kiyokawa H, LaRusso NF: Inhibition of Cdc25A suppresses hepato-renal cystogenesis in rodent models of polycystic kidney and liver disease. Gastroenterology 2012, 142:622–633.e624
27. Lee SO, Masyuk T, Splinter P, Banales JM, Masyuk A, Stroope A, Larusso N: MicroRNA15a modulates expression of the cell-cycle regulator Cdc25A and affects hepatic cystogenesis in a rat model of polycystic kidney disease. J Clin Invest 2008, 118:3714–3724
28. Bartel DP: MicroRNAs: target recognition and regulatory functions. Cell 2009, 136:215–233
29. Vigo E, Muller H, Prosperini E, Hateboer G, Cartwright P, Moroni MC, Helin K: CDC25A phosphatase is a target of E2F and is required for efficient E2F-induced S phase. Mol Cellular Biol 1999, 19:6379–6395
30. Elmen J, Lindow M, Schutz S, Lawrence M, Petri A, Obad S, Lindholm M, Hedtjarn M, Hansen HF, Berger U, Gullans S, Kearney P, Sarnow P, Straarup EM, Kauppinen S: LNA-mediated microRNA silencing in non-human primates. Nature 2008, 452:896–899
31. Esau C, Davis S, Murray SF, Yu XX, Pandey SK, Pear M, Watts L, Booten SL, Graham M, McKay R, Subramaniam A, Propp S, Lollo BA, Freier S, Bennett CF, Bhanot S, Monia BP: miR-122 regulation of lipid metabolism revealed by in vivo antisense targeting. Cell Metab 2006, 3:87–98
32. Li Y, Ye X, Tan C, Hongo JA, Zha J, Liu J, Kallop D, Ludlam MJ, Pei L: Axl as a potential therapeutic target in cancer: role of Axl in tumor growth, metastasis and angiogenesis. Oncogene 2009, 28:3442–3455
33. Archer MC: Mechanisms of action of N-nitroso compounds. Cancer Surv 1989, 8:241–250
34. Thompson MD, Wickline ED, Bowen WB, Lu A, Singh S, Misse A, Monga SP: Spontaneous repopulation of beta-catenin null livers with beta-catenin-positive hepatocytes after chronic murine liver injury. Hepatology 2011, 54:1333–1343
35. Vachha B, Sun MR, Siewert B, Eisenberg RL: Cystic lesions of the liver. AJR Am J Roentgenol 2011, 196:W355–W366
36. Kushida M, Kamendulis LM, Peat TJ, Klaunig JE: Dose-related induction of hepatic preneoplastic lesions by diethylnitrosamine in C57BL/6 mice. Toxicol Pathol 2011, 39:776–786
37. Umemura T, Kodama Y, Kanki K, Iatropoulos MJ, Nishikawa A, Hirose M, Williams GM: Pentachlorophenol (but not phenobarbital) promotes intrahepatic biliary cysts induced by diethylnitrosamine to cholangio cystic neoplasms in B6C3F1 mice possibly due to oxidative stress. Toxicol Pathol 2003, 31:10–13
38. Sun B, Karin M: Inflammation and liver tumorigenesis. Front Med 2013, 7:242–254
39. Eltzschig HK, Eckle T: Ischemia and reperfusion: from mechanism to translation. Nat Med 2011, 17:1391–1401
40. Wallace KL, Linden J: Adenosine A2A receptors induced on iNKT and NK cells reduce pulmonary inflammation and injury in mice with sickle cell disease. Blood 2010, 116:5010–5020
41. Eckle T, Faigle M, Grenz A, Laucher S, Thompson LF, Eltzschig HK: A2B adenosine receptor dampens hypoxia-induced vascular leak. Blood 2008, 111:2024–2035
42. Hebert C, Norris K, Scheper MA, Nikitakis N, Sauk JJ: High mobility group A2 is a target for miRNA-98 in head and neck squamous cell carcinoma. Mol Cancer 2007, 6:5
43. Chu AS, Friedman JR: A role for microRNA in cystic liver and kidney diseases. J Clin Invest 2008, 118:3585–3587
44. Janssen MJ, Salomon J: Te Morsche RH, Drenth JP: Loss of heterozygosity is present in SEC63 germline carriers with polycystic liver disease. PLoS One 2012, 7:e50324
45. Banales JM, Munoz-Garrido P, Bujanda L: Somatic second-hit mutations leads to polycystic liver diseases. World J Gastroenterol 2013, 19:141–143
46. O'Bryan JP, Frye RA, Cogswell PC, Neubauer A, Kitch B, Prokop C, Espinosa R 3rd, Le Beau MM, Earp HS, Liu ET: axl, a transforming gene isolated from primary human myeloid leukemia cells, encodes a novel receptor tyrosine kinase. Mol Cell Biol 1991, 11:5016–5031
47. Verma A, Warner SL, Vankayalapati H, Bearss DJ, Sharma S: Targeting Axl and Mer kinases in cancer. Mol Cancer Ther 2011, 10:1763–1773